S.M. acknowledges the NRCC for a graduate scholarship.

Registry No. V, 7440-62-2; CH_4, 74-82-8; C_2H_6, 74-84-0; C_3H_8, 74-98-6; C_4H_{10}, 106-97-8; C_5H_{12}, 109-66-0; C_6H_{14}, 110-54-3; C_7H_{16}, 142-82-5; C_8H_{18}, 111-65-9; C_9H_{20}, 111-84-2; $C_{10}H_{22}$, 124-18-5; cyclopentane, 287-92-3; 2-methylbutane, 78-78-4; cyclohexane, 110-82-7; 2-methylpentane, 107-83-5; 2,3-dimethylbutane, 79-29-8; cycloheptane, 291-64-5; 2-methylhexane, 591-76-4; 2,3-dimethylpentane, 565-59-3; cyclopropane, 75-19-4; cyclooctane, 292-64-8; Ar, 7440-37-1.

References and Notes

(1) (a) D. Gruen in "Cryochemistry", M. Moskovits and G. A. Ozin, Ed., Wiley, New York, N.Y., 1976; (b) D. M. Mann and H. P. Broida, *J. Chem. Phys.*, **55**, 84 (1971); (c) W. Klotzbücher and G. A. Ozin, *Inorg. Chem.*, **15**, 292 (1975); (d) O. M. Kolb, D. Leutloff, and W. Schulze, *J. Chem. Phys.*, **66**, 2806 (1977), and references cited therein.

(2) (a) J. D. McCullough and W. W. Duley, *Spectrosc. Lett.*, **8**, 51 (1975); (b) W. R. M. Graham and W. W. Duley, *J. Chem. Phys.*, **55**, 2527 (1971).

(3) (a) K. J. Klabunde, H. F. Efner, T. O. Murdock, and R. Ropple, *J. Am. Chem. Soc.*, **98**, 1021 (1976); (b) K. J. Klabunde, H. F. Efner, L. Satek, and W. Duley, *J. Organomet. Chem.*, **71**, 309 (1974).

(4) (a) T. A. Ford, H. Huber, W. Klotzbücher, E. P. Kündig, M. Moskovits, and G. A. Ozin, *J. Chem. Phys.*, **66**, 524 (1977); (b) M. Moskovits and J. Hulse, *J. Chem. Soc., Faraday Trans. 2*, 471 (1977).

(5) M. Moskovits and G. A. Ozin, *Appl. Spectrosc.*, **26**, 481 (1972); E. P. Kündig, M. Moskovits, and G. A. Ozin, *J. Mol. Struct.*, **14**, 137 (1972).

(6) H. E. Hallam and G. F. Scrimshaw in "Vibrational Spectroscopy of Trapped Species", H. E. Hallam, Ed., Wiley-Interscience, New York, N.Y., 1973, Chapter 2.

(7) D. H. W. Carstens, W. Braschear, O. R. Eslinger, and D. M. Gruen, *Appl. Spectrosc.*, **26**, 184 (1972).

Contribution from the Lash Miller Chemistry Laboratories and Erindale College,
The University of Toronto, Toronto, Ontario, Canada

Cryochemical Studies of Zerovalent Copper–Ethylene Complexes, $(C_2H_4)_nCu$ and $(C_2H_4)_mCu_2$ (Where $n = 1–3$; $m = 4$ or 6), and Their Use in Forming Copper Clusters. Localized Bonding Models for Ethylene Chemisorption onto Bulk Copper

GEOFFREY A. OZIN,* HELMUT HUBER, and DOUGLAS McINTOSH

Received June 1, 1977 AIC70395K

Cryochemical reactions of copper atoms with ethylene and ethylene/argon mixtures at 10–12 K using copper concentration conditions which favor *mononuclear* reaction products give rise to a series of three, highly colored, binary copper–ethylene complexes. Vibrational and electronic spectroscopy taken in conjunction with copper/ethylene/argon concentration experiments, $^{12}C_2H_4/^{13}C_2H_4/Ar$ mixed isotope substitution studies, and comparisons with $(C_2H_4)_nCo$ and $(C_2H_4)_nNi$ (where $n = 1–3$) provide strong evidence in support of a similar $(C_2H_4)_nCu$ formulation. Particularly noteworthy properties of these copper–ethylene complexes concern their marked *instability* relative to their respective nickel complexes, although this is thought to be partly a manifestation of their paramagnetic character and tendency toward dimerization. Electronically, the $(C_2H_4)_nCu$ complexes comprise a unique series in that they *all* display intense *visible* and *ultraviolet* charge-transfer absorptions which monotonically *red* and *blue* shift respectively with increasing ethylene stoichiometry. These spectral trends when taken together with the available electronic spectral data for copper(I)–ethylene complexes as well as the results of semiempirical molecular orbital calculations for $(C_2H_4)_nCu$ allow a reasonable assignment of the visible and ultraviolet charge-transfer bands to be made. Quantitative Cu/C_2H_4 concentration experiments and controlled annealing (30–45 K) of matrices containing $(C_2H_4)_nCu$ (where $n = 2, 3$) provide convincing evidence for a transformation to $(C_2H_4)_mCu_2$ (where $m = 4$ or 6). Especially interesting is the observation that thermal annealing of $(C_2H_4)_mCu_2$ in the higher temperature range 45–100 K seems to present a route to small, copper clusters. Finally, the value of these mononuclear and binuclear copper–ethylene complexes as localized bonding representations for ethylene chemisorbed onto bulk copper is briefly contemplated in the light of recent ultraviolet photoemission spectra for ethylene chemisorbed onto copper surfaces.

Introduction

While it is true that a wide variety of copper(I)–olefin complexes are known,[1] some of which are catalysts for photochemical reactions of alkenes,[2] there are no known examples of room temperature, stable, zerovalent copper–olefin complexes. One must presume that this is a manifestation of the weakness of copper(0)–olefin interactions and in a localized bonding sense[3] mirrors the poor chemisorptive capacity of bulk copper for alkenes at room temperature.[4] In this paper we report synthetic, vibrational, and electronic information for $(C_2H_4)_nCu$ and $(C_2H_4)_mCu_2$ (where $n = 1–3$; $m = 4$ or 6) noting that a brief report of the mononuclear complexes has already been presented.[5] The use of these complexes as "chemisorption models" for ethylene bonded to copper surfaces,[3,4] as well as an interesting new source of small copper clusters,[25] is carefully assessed.

Experimental Section

Monatomic copper was generated by directly heating a thin tungsten rod (0.025 in.) around the center of which was wound copper wire (0.005 in.). The copper metal (99.99%) was supplied by McKay, New York, N.Y., Research grade $^{12}C_2H_4$ (99.90%) was supplied by Matheson of Canada and $^{13}C_2H_4$ (95%) by Stohler Isotopes, Montreal. The furnace used for the evaporation of the metals has been described previously.[6] The rate of copper atom deposition was continuously monitored using a quartz crystal microbalance.[6] In the infrared experiments, matrices were deposited on either a NaCl or CsI plate cooled to 10 K by means of an Air Products Displex closed cycle helium refrigerator. Infrared spectra were recorded on a Perkin-Elmer 180 spectrophotometer. Ultraviolet–visible spectra were recorded on a standard Varian Techtron instrument in the range 190–900 nm, the sample being deposited on a NaCl optical plate. Extended Hückel molecular orbital calculations were run on an IBM 370 computer.

Results and Discussion

In a preliminary report[5] we recently communicated the observation that the reaction between copper atoms and ethylene at 10–12 K leads not only to monoethylene copper $(C_2H_4)Cu$ (**13e**) but also to $(C_2H_4)_2Cu$ (**15e**) (which at the time represented the first example of a binary bis(ethylene) transition-metal complex) and $(C_2H_4)_3Cu$ (**17e**), which can be considered to be the next highest member of the series $(C_2H_4)_3Co$ (**15e**),[7] $(C_2H_4)_3Ni$ (**16e**).[8] However, these conclusions were based only on copper/ethylene/argon concentration studies as monitored by matrix infrared spectroscopy.[5]

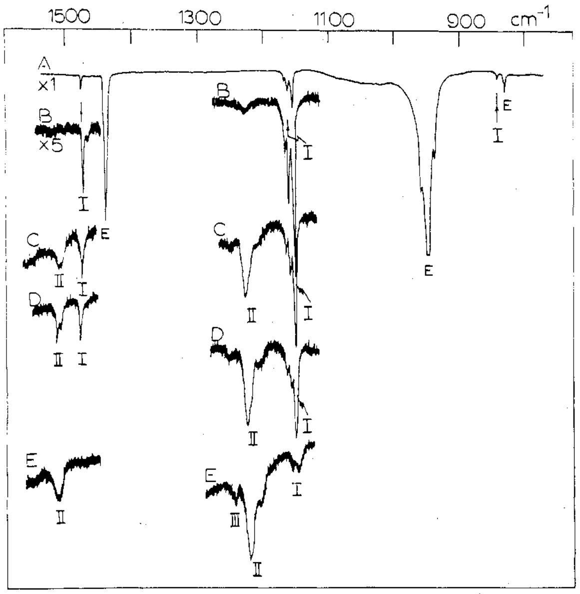

Figure 1. The matrix infrared spectra of the products of the cocondensation reaction of atomic copper with (A) $^{12}C_2H_4/Ar \simeq 1/100$, (B) the same as (A) but with 5× scale expansion, (C) to (E) the effect of warming the matrix to 20, 25, and 30 K, respectively, showing the characteristic growth and decay patterns of $(C_2H_4)_2Cu$ (II) and $(C_2H_4)Cu$ (I). Note that a trace amount of $(C_2H_4)_3Cu$ (III) only begins to appear at 30 K. Under these experimental conditions, higher temperature annealing experiments cause preferential dimerization and/or decomposition rather than formation of III. (E) denotes the absorptions of unreacted $^{12}C_2H_4$ in the matrix.

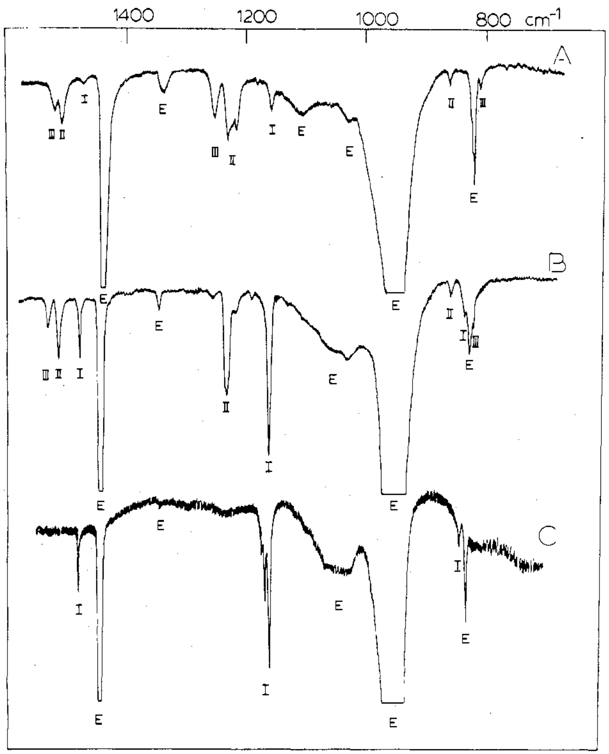

Figure 2. The matrix infrared spectra of the products of the cocondensation reaction of atomic copper with (A) $^{12}C_2H_4$, (B) $^{12}C_2H_4/Ar \simeq 1/10$, and (C) $^{12}C_2H_4/Ar \simeq 1/100$ at 10–12 K showing the characteristic absorptions of $(C_2H_4)_3Cu$ (III), $(C_2H_4)_2Cu$ (II), and $(C_2H_4)Cu$ (I) in the ν(C=C) stretching (1520–1450 cm^{-1}), δ (CH_2) deformational (1250–1100 cm^{-1}), and $\rho_w(CH_2)$ wagging (900–800 cm^{-1}) regions.

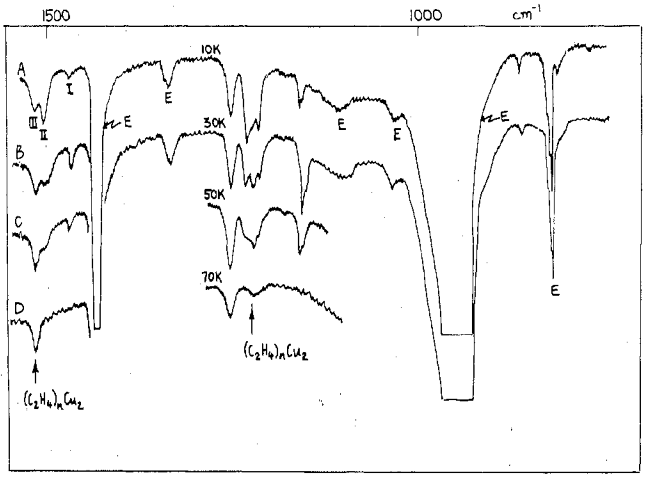

Figure 3. The matrix infrared spectrum of the products of the cocondensation reaction of copper atoms with pure $^{12}C_2H_4$ (A) at 10–12 K and (B–D) showing the effects of warming the matrix to 30, 50, and 70 K at which temperatures the corresponding ultraviolet–visible spectra show decay of all mononuclears with the concomitant formation of a binuclear copper–copper bonded complex $(C_2H_4)_nCu_2$ (where n = 4 or 6). See text.

Since this brief exposure to zerovalent copper–olefin chemistry, we have performed detailed vibrational isotope substitution experiments with $^{12}C_2H_4/^{13}C_2H_4/Ar$ mixtures, the results of which provide convincing support for our original stoichiometric assignments particularly for the mono and bis complexes. Furthermore, we have managed to collect electronic spectral data for each of these binary copper–ethylene fragments and are now in a position to rationalize vibrational, electronic, and geometric trends within the series. An extension to the interesting binuclear species $(C_2H_4)_mCu_2$ (where m = 4 or 6) has also been achieved. In what follows we will formalize the experimental data.

Infrared Experiments. Mononuclears. When copper atoms are cocondensed with $^{12}C_2H_4/Ar \simeq 1/100$ at 10–12 K (using very low concentrations of Cu to eliminate complications due to cluster formation, $Cu/Ar \simeq 1/10^4$) aside from infrared absorptions belonging to free ethylene isolated in the Ar matrix (labelled E in the figures) new absorptions are observed at 3120, 1475, 1164/1155,[32] and 840 cm^{-1} (Figure 1A and B). On warming the matrix to 30–35 K this set of absorptions gradually diminishes in intensity but maintains the same relative intensity pattern throughout the annealing process. A number of experiments along these lines suggests that these absorptions are associated with a single, low ethylene stoichiometry complex which we denote as I. Meanwhile, during these warming experiments a new set of absorptions is observed to grow in at 1505, 1228, and 862 cm^{-1} (Figure 1C–E) these too maintaining the same relative intensities and are ascribed to a second copper–ethylene species denoted II.

In matrices which are more heavily doped with ethylene, $^{12}C_2H_4/Ar \simeq 1/10$, the group of absorptions associated with species I and II both appear on deposition (Figure 2B) with comparable intensities, together with some slight indication of new lines at 1525, 1252 and 810 cm^{-1}, possibly belonging to a third species denoted III. On warming these 1/10 matrices in the range 10–35 K the lines belonging to species I gradually diminish in intensity (that is, paralleling the behavior observed in 1/100 matrices), leaving behind species II as the major absorbing species in the infrared spectrum.[31]

That a third species III exists in the Cu/C_2H_4 system is best seen from experiments in which Cu atoms are cocondensed with pure C_2H_4 at 10–12 K (Figure 2A). The infrared spectrum on deposition shows trace amounts of species I and comparable quantities of species II and III, the latter being associated with absorptions at 1517, 1252, and 810 cm^{-1}. On warming these matrices to 30–35 K one finds that species II

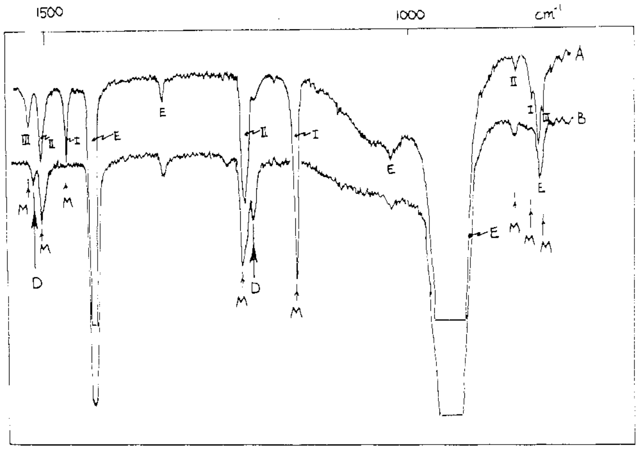

Figure 4. Matrix infrared spectrum of the products of the cocondensation reaction of Cu atoms with concentrated $^{12}C_2H_4/Ar \simeq 1/10$ mixtures (A) at 10–12 K and (B) after warm-up to 40–50 K showing the growth of new $\nu(CC)$ stretching and $\delta(CH_2)$ deformational modes labeled D which from the corresponding ultraviolet–visible experiments appear to be best assigned to a binuclear, copper–copper bonded complex, $(C_2H_4)_nCu_2$ (where n = 4 or 6).

Table I. Infrared Spectra for Binary Zerovalent Transition Metal-Ethylene Complexes

$(C_2H_4)Cu$	$(C_2H_4)Ag$[10]	$(C_2H_4)Au$[10]	Approx description of mode[a]
1475 1156/1138	1476 1152/1132	1476 1144/1135	$\nu(CC)$ or $\delta(CH_2)$
840	794	890	$\rho_w(CH_2)$
$(C_2H_4)_3Co$[7]	$(C_2H_4)_3Ni$[8b]	$(C_2H_4)_3Cu$	
1499 1225	1510 1244	1517 1252	$\nu(CC)$ or $\delta(CH_2)$
		810	$\rho_w(CH_2)$
$(C_2H_4)Cu$	$(C_2H_4)_2Cu$	$(C_2H_4)_3Cu$	
1475 1156/1138	1505 1228	1525 1252	$\nu(CC)$ or $\delta(CH_2)$
840	862	810	$\rho_w(CH_2)$

[a] It is quite likely that these modes are highly coupled. Calculations are in progress with the $(^{12}C_2H_4)Ag$, $(^{13}C_2H_4)Ag$, $(^{12}C_2D_4)Ag$, $(^{13}C_2D_4)Ag$ system to establish the extent of this vibrational coupling (ref 30).

and III dominate.[31] However, at higher temperatures some subtle spectral changes ensue in the $\nu(CC)$ and $\delta(CH_2)$ regions (Figure 3), which together with similar effects in concentrated $^{12}C_2H_4/Ar \simeq 1/10$ matrices (Figure 4) leads one to suspect the possibility of further complex formation.

As it turns out the corresponding ultraviolet–visible spectral changes (described later on) are considerably more definitive in this respect and provide convincing evidence in favor of a dimerization process in which paramagnetic $(C_2H_4)_nCu$ fragments diffuse and aggregate to form $(C_2H_4)_mCu_2$ binuclear complexes (where n is thought to be 4 or 6).

Returning to the discussion of the *three* mononuclear reaction products, one is led to the a priori assignment $(C_2H_4)Cu$ (I), $(C_2H_4)_2Cu$ (II), and $(C_2H_4)_3Cu$ (III). Support for the monoethylene copper formulation I stems from the remarkably close similarity of its infrared spectrum to those of $(C_2H_4)Ag$[10] and $(C_2H_4)Au$[10] shown in Table I. The tris(ethylene) formulation for the highest stoichiometry product is reinforced by the close correspondence with the infrared spectra of the 15- and 16-electron tris(ethylene) complexes[7,8] $(C_2H_4)_3Co$ and $(C_2H_4)_3Ni$ also shown in Table I. The 17-electron $(C_2H_4)_3Cu$ complex can be considered to be the next highest member of this series, which is in keeping with the observed trend of increasing C═C bond strength (as measured by $\nu(C{=}C)$ in Table I) on passing from $(C_2H_4)_3Co$ to $(C_2H_4)_3Cu$. This is certainly in line with the idea of decreasing $M(d\pi) \rightarrow C_2H_4(\pi^*)$ charge transfer on moving from the elements on the left of the first transition series to those on the right.

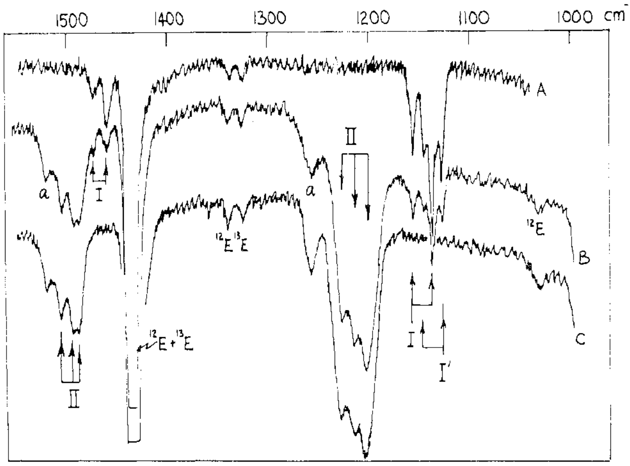

Figure 5. The matrix infrared spectra of the products of the cocondensation reaction of Cu atoms with $^{12}C_2H_4/^{13}C_2H_4/Ar \simeq 1/2/100$ (A) at 10–12 K, (B) after warm-up to 20–25 K, and (C) after warm-up to 30 K showing the characteristic $^{12}C/^{13}C$ isotope patterns in the $\nu(C{=}C)$ stretching and $\delta(CH_2)$ deformational regions for monoethylenecopper and bis(ethylene)copper, labeled I and II, respectively (I′ represents a matrix site or multiple trapping site splitting and "a" denotes a trace amount of tris(ethylene)copper).

Table II. Isotope Substitution Data for $(^{12}C_2H_4)_n(^{13}C_2H_4)_{m-n}Cu$ (where $m = 2, n = 0, 1, 2; m = 1, n = 0, 1$)

$^{12}C_2H_4/Ar$	$^{13}C_2H_4/Ar$	$^{12}C_2H_4/$ $^{13}C_2H_4/Ar$	Mode assignment[a]	Molecule assignment[c]
1505		1505	$\nu(C{=}C)$	$(^{12}C_2H_4)_2Cu$
		1493	$\nu(C{=}C)$	$(^{12}C_2H_4)(^{13}C_2H_4)Cu$
	1488	1488	$\nu(C{=}C)$	$(^{13}C_2H_4)_2Cu$
1475		1475	$\nu(C{=}C)$	$(^{12}C_2H_4)Cu$
	1460	1460	$\nu(C{=}C)$	$(^{13}C_2H_4)Cu$
1228		1228	$\delta(CH_2)$	$(^{12}C_2H_4)_2Cu$
		1216	$\delta(CH_2)$	$(^{12}C_2H_4)(^{13}C_2H_4)Cu$
	1204	1204	$\delta(CH_2)$	$(^{13}C_2H_4)_2Cu$
1156/1138[b]		1156/1138[b]	$\delta(CH_2)$	$(^{12}C_2H_4)Cu$
	1145/1126[b]	1145/1126[b]	$\delta(CH_2)$	$(^{13}C_2H_4)Cu$

[a] It is quite likely that the $\nu(C{=}C)$ and $\delta(CH_2)$ modes are highly coupled (see ref 28). [b] Matrix site or multiple trapping site effect: variable component intensities depending on the Cu/C_2H_4/Ar concentration and deposition conditions. [c] Units in cm^{-1}.

The close resemblence of the infrared spectra of $(C_2H_4)_3M$ (where M = Co, Ni, Cu) would also tend to indicate that the complexes are isostructural, probably with a planar D_{3h} geometry by analogy with the crystallographically established planar geometries for $(C_2H_4)_2(C_2F_4)Pt$[11] and tris(bicyclo[2.2.1]heptene)M (where M = Ni, Pd, Pt)[12] as well as the theoretically predicted D_{3h} planar, minimum-energy configuration for $(C_2H_4)_3Ni$.[13]

Infrared Isotope Substitution Experiments. We have recently demonstrated with the Pd/C_2H_4 system that mixed $^{12}C_2H_4/^{13}C_2H_4/Ar$ experiments are capable of generating isotopic patterns characteristic of the ethylene stoichiometry.[14] In the context of the present Cu/C_2H_4 investigations the suspected mono- and bis(ethylene) complexes appear to be ideally suited for isotopic studies particularly in the $\nu(CC)$ stretching and $\delta(CH_2)$ deformational regions of the infrared spectrum.

Table III. Ultraviolet-Visible Absorption Spectra of Binary Ethylene Complexes of Copper(0), $(C_2H_4)_nCu$ (where n = 1-3)

C_2H_4/Ar (1/25 to 1/50) (10-12 K)	C_2H_4/Ar (1/10) (10-12 K)	C_2H_4 pure (10-12 K)	Molecule assignment	Optical assignment
$486^{a,b}$	$492^{a,b}$	$504^{a,b}$ (s)	$(C_2H_4)_3Cu$	ML to MLCT[d]
$480^{a,b}$	$486^{a,b}$	$483^{a,b}$ (wsh)	$(C_2H_4)_2Cu$	ML to MLCT[d]
420^{b}			$(C_2H_4)Cu$	ML to MLCT[d]
382^{b}			$(C_2H_4)Cu$	MLCT
368^{b}	368^{b}		$(C_2H_4)_2Cu$	
353^{b}	356^{b}	358^{b} (w)	$(C_2H_4)_3Cu$	
	$345/342^{c}$	$347/342^{c}$ (vw)		
276^{b}	273^{b}	280^{b} (wbr)	$(C_2H_4)_2Cu$	MLCT
235^{b}	230^{b}	231^{b} (m)	$(C_2H_4)_3Cu$	MLCT

[a] Broad, because of a suspected overlap of the visible bands of $(C_2H_4)_2Cu$ and $(C_2H_4)_3Cu$; shows expected shift of λ_{max} on warming to 30–32 K. [b] Absorptions which show parallel growth and decay behavior during warm-up experiments in the 10–35 K range. [c] Possibly one of the $^2S \rightarrow {}^2P_{3/2,1/2}$ crystal field split, spin-orbit couplets (ref 29). [d] See text for an explanation of these assignments.

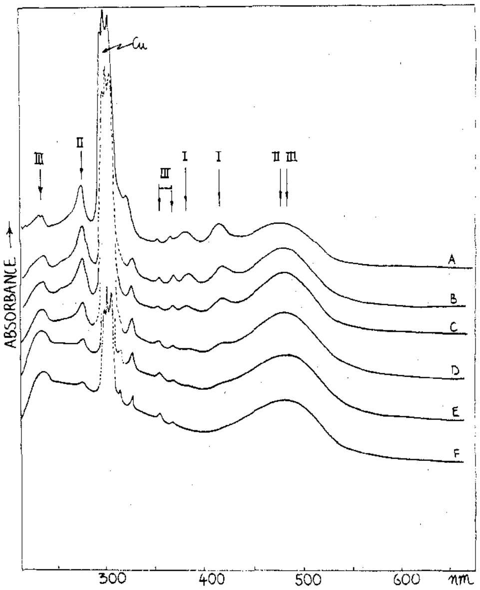

Figure 6. The matrix ultraviolet–visible spectra of the products of the cocondensation reaction of Cu atoms with $^{12}C_2H_4/Ar \simeq 1/25$ (A) at 10–12 K and (B–F) after successive warm-up experiments to 15, 20, 25, 30, and 35 K showing the growth and decay patterns of the ultraviolet and visible absorptions characteristic of $(C_2H_4)Cu$ (I), $(C_2H_4)_2Cu$ (II), and $(C_2H_4)_3Cu$ (III). The presence of some unreacted atomic copper in the matrix is indicated by Cu.

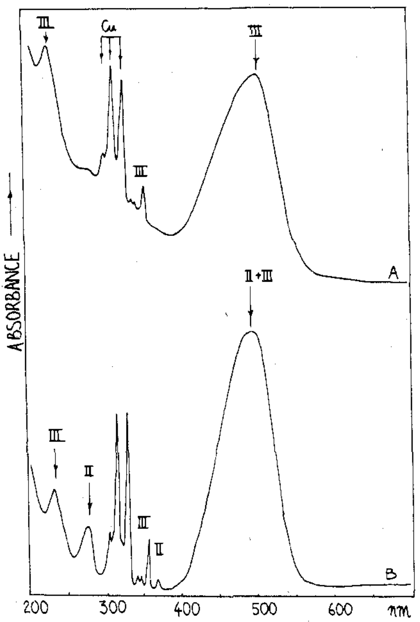

Figure 7. The matrix ultraviolet–visible spectra of the products of the cocondensation reaction of Cu atoms with (A) $^{12}C_2H_4$ and (B) $^{12}C_2H_4/Ar \simeq 1/10$ at 10–12 K showing the characteristic ultraviolet and visible absorptions of $(C_2H_4)_3Cu$ (III) and $(C_2H_4)_2Cu$ (II). The presence of some unreacted atomic copper in the matrix is indicated by Cu.

A typical series of $^{12}C_2H_4/^{13}C_2H_4/Ar \simeq 1/2/100$ mixed isotope experiments is illustrated in Figure 5 and summarized in Table II. Under high dilution conditions and 10-12 K deposition temperatures the ν(C=C) stretching mode of the suspected monoethylene complex I appears as an isotopic doublet (Figure 5A) at 1475/1460 cm^{-1}. In keeping with this, the matrix split $\delta(CH_2)$deformational mode also appears as an isotopic *doublet* (Figure 5A) at 1156/1138 and 1145/1126 cm^{-1} and therefore provides unequivocal evidence in favor of the $(C_2H_4)Cu$ formulation for I. Similar considerations apply to the ν(C=C) stretching and $\delta(CH_2)$ deformational modes of the proposed bis(ethylene) complex II. By annealing these $^{12}C_2H_4/^{13}C_2H_4/Ar \simeq 1/2/100$ matrices to 20–30 K, the isotopic pattern of I gradually decays concomitant with the growth of the corresponding isotopic structure for species II. Figure 5B,C illustrates this point from which one can discern *triplet* isotopic structure for the ν(C=C) stretching mode 1505/1493/1488 cm^{-1} as well as for the $\delta(CH_2)$ deformational mode 1228/1216/1204 cm^{-1}, precisely the patterns expected for a $(C_2H_4)_2Cu$ formulation for II. These isotopic and stoichiometric assignments receive additional support from the corresponding $^{13}C_2H_4/Ar$ experiments which place ν(C=C) and $\delta(CH_2)$ for $(^{13}C_2H_4)Cu$ at 1460/1145/1126 cm^{-1} and $(^{13}C_2H_4)_2Cu$ at 1488/1204 cm^{-1} (Table II). The difficulty of generating the suspected tris(ethylene) complex III in the absence of II, together with the complications of isotopic band overlap, precluded an unambiguous stoichiometric assignment for $(C_2H_4)_3Cu$, although there can be little doubt from our experiments and comparisons with other tris(ethylene) complexes that our formulation of III is correct.[31]

Ultraviolet-Visible Experiments. Mononuclears. Using similar procedures to those described for the infrared experiments, the corresponding electronic spectral data were collected, whenever possible, from the same matrix sample. The characteristic absorptions for I, II, and III could be easily discerned from their relative intensity behavior as a function of the $Cu/C_2H_4/Ar$ ratio as well as their growth and decay patterns as a function of annealing temperature for each matrix studied. These data are summarized in Table III and Figures 6 and 7.

By working with dilute and concentrated C_2H_4/Ar matrices one can immediately identify *three* sets of absorptions characteristic of the *three* mononuclear complexes I, II, and III. Of particular note is the identification of *one* intense visible absorption for each complex which monotonically *red* shifts with increasing ethylene stoichiometry. In addition, *one*

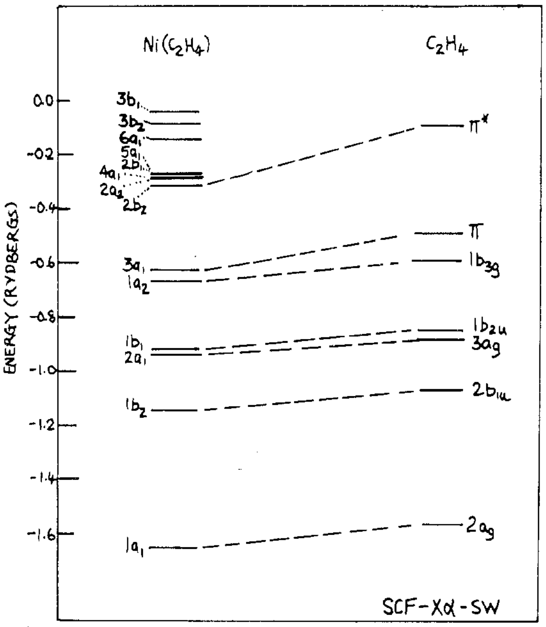

Figure 8. Comparison of the calculated SCF-Xα-SW energy levels for $(C_2H_4)Ni$ and C_2H_4 as taken from ref 16.

intense ultraviolet absorption can be associated with each complex but with the *opposite* effect of blue shifting with increasing ethylene stoichiometry. Our assignments are listed in Table III.

A number of features of these optical spectra are particularly significant. To begin, the corresponding data for $(C_2H_4)_nNi$[8b] and $(C_2H_4)_nPd$[14] also display *one* intense ultraviolet absorption per complex which similarly *blue* shifts with increasing ethylene stoichiometry. Moreover, the copper(I)–ethylene cation[15b] $[(C_2H_4)Cu]^+$, which is isoelectronic with $(C_2H_4)Ni$, also displays a single, intense ultraviolet absorption which is *blue* shifted with respect to both $(C_2H_4)Cu$ and $(C_2H_4)Ni$.

Complex	nm	Complex	nm
$(C_2H_4)_3Ni$	230	$(C_2H_4)_3Cu$	235
$(C_2H_4)_2Ni$	250	$(C_2H_4)_2Cu$	276
$(C_2H_4)Ni$	280	$(C_2H_4)Cu$	382
$[(C_2H_4)Cu]^+$	228		

For the purposes of this discussion we have summarized Messmer's Xα-SW molecular orbital calculations[16] for $(C_2H_4)Ni$ and C_2H_4 in Figure 8. Related orbitals are connected by broken lines, from which it can be seen that the ethylene orbitals from $2a_g$ up to $1b_{3g}$ undergo an almost uniform shift when ethylene interacts with a single nickel atom. The π and π^* levels of ethylene on the other hand are seen to experience a rather marked change on interacting with a nickel atom, where the $2b_2$ and $3a_1$ orbitals of Figure 8 are primarily responsible for bonding. The $2b_1$, $4a_1$, and $2a_2$ orbitals are essentially nonbonding atomic Ni 3d orbitals in nature and the energy levels are filled up to and including $5a_1$. A similar pattern of levels is expected for the $(C_2H_4)Cu$ system except that the extra electron in Messmer's scheme is likely to reside in the $6a_1$ orbital.[37] As it turns out, the energy level scheme calculated by us for $(C_2H_4)Cu$, within the framework and approximations of extended Hückel theory, apart from underestimating d-orbital splittings, is remarkably similar to Messmer's Xα-SW orbital scheme.[16,37] The only noticeable difference is an inversion of the ordering of the $6a_1/3b_2$ orbital energies (Figure 9; note that low-lying, ethylene-based orbitals are not included in this figure).

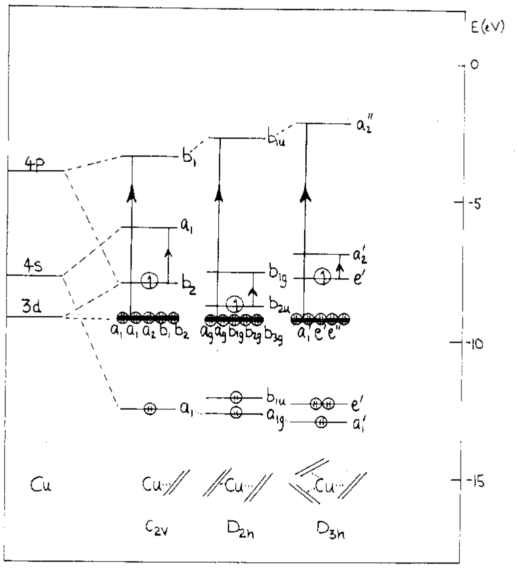

Figure 9. Extended Hückel molecular orbital energy level schemes for C_{2v} $[(C_2H_4)Cu]$, D_{2h} $[(C_2H_4)_2Cu]$, and D_{3h} $[(C_2H_4)_3Cu]$ showing trends in certain electric-dipole, spin-allowed electronic transitions which parallel the behavior observed for the *blue* shifting ultraviolet absorption yet *red* shifting visible absorption with *increasing* ethylene stoichiometry (see text and tables for details).

Table IV. Parameters[a] Used in the Extended Hückel Molecular Orbital Calculations of $(C_2H_4)_nCu$ (where n = 1-3)

	Orbital	Orbital exponent[b]	VOIP, eV
Cu[b]	3d	4.400	−9.23
	4s	1.461	−7.72
	4p	1.461	−3.94
C	2s	1.608	−19.42
	2p	1.568	−10.64
H	1s	1.000	−13.60

[a] CC bond length, 1.40 Å; CuC bond length, 2.08 Å. [b] Taken from ref 23.

Table V. "Trends" in the Observed and Extended Hückel Estimated Transition Energies (eV) for the Intense Visible and Ultraviolet Absorptions of $(C_2H_4)_nCu$ (where n = 1-3)[c]

Visible absorption[b]		UV absorption[a]		
Obsd	Calcd	Obsd	Calcd	Molecule
2.95	2.09	3.25	5.88	$(C_2H_4)Cu$
2.58	1.25	4.54	6.49	$(C_2H_4)_2Cu$
2.45	0.92	5.28	7.08	$(C_2H_4)_3Cu$

[a] Probably best described as metal to metal-ligand charge-transfer transition. [b] Probably best described as metal-ligand to metal-ligand charge-transfer transition. [c] Recent SCF-Xα-SW, spin-restricted transition-state calculations generally support the conclusions arrived at through EHMO techniques.[37]

By comparison with the optical spectra of known transition-metal olefin complexes[17] and by consultation with the results of the Xα-SW calculations[16] for $(C_2H_4)Ni$ and extended Hückel calculations of $(C_2H_4)Cu$ (Figures 8 and 9 and Tables IV and V) one can tentatively ascribe the 280- and 382-nm absorptions of $(C_2H_4)Ni$ and $(C_2H_4)Cu$ respectively to an electronic transition from the filled metal d shell to an empty metal–ethylene type combination, that is, MLCT in character.[37] Credence for this assignment originates from two other sources. First, these absorptions *blue* shift to 228 nm[15b] on passing to $[(C_2H_4)Cu]^+$ in line with the anticipated stabilization of the closed 3d shell of Cu(I) with respect to both Cu(0) and Ni(0). Second, the monotonic *blue* shifting of the observed ultraviolet bands of $(C_2H_4)_nM$ with increasing ethylene stoichiometry is essentially reproduced for the MLCT transitions calculated by extended Hückel procedures, illustrated schematically in Figure 9 and tabulated in Table V.[37]

Electronically, the $(C_2H_4)_nCu$ complexes are unique in that they *all* display very intense, *visible*, charge-transfer absorptions which as noted earlier monotonically *red* shift with increasing ethylene stoichiometry. The absence of such absorptions for the corresponding $(C_2H_4)_nNi$ series immediately associates the visible bands of $(C_2H_4)_nCu$ with *excitation of the unpaired electron.* In the context of our extended Hückel analysis of $(C_2H_4)_nCu$ (where $n = 1-3$) the transitions indicated in Figure 9 mirror the trend in transition energies for the visible absorptions (Table V) and from the orbital descriptions are probably best described as excitations between levels which have mixed metal–ligand character and are charge transfer in nature.[37] This proposal is certainly consistent with the absence of visible charge transfer[15b] in $[(C_2H_4)Cu]^+$.

Ultraviolet–Visible Experiments. Binuclears. Earlier in our discussions we alluded to the possibility that binuclear copper–ethylene complexes might be generated from the dimerization of mononuclear copper–ethylene fragment molecules. If this is indeed possible, one would also envisage that quantitative copper/ethylene concentration experiments could also provide a definitive pathway to similar types of $(C_2H_4)_mCu_2$ cluster complexes.[9] By working in concentrated C_2H_4/Ar mixtures and/or pure C_2H_4 one might hope to generate $(C_2H_4)_4Cu_2$ and/or $(C_2H_4)_6Cu_2$. Such clusters may be considered to be useful localized bonding models for surface reaction intermediates under "high coverage" bulk chemisorption conditions.

Recall that small, well-defined naked Cu_n clusters can be generated in argon matrices in varying amounts depending on the Cu/Ar ratio and deposition temperature.[18,19] At least two electronic transitions of Cu_2 have been identified by quantitative ultraviolet–visible, copper-concentration experiments.[18,19] Electronic absorptions suspected to belong to Cu_3 occur in similar spectral regions to those of Cu_2 (230–270/380–440 nm as seen from high copper concentration experiments); however, band overlap problems preclude a definitive identification of Cu_3 at the time of writing although we note that Ag_3 (which is expected to be electronically very similar to Cu_3) in Ar, Kr, Xe, and CH_4 matrices has recently been shown to absorb in the ranges 230–260 and 420–440 nm.[38,39] Suffice it to say that with the prior knowledge that Cu atoms and Cu/Cu_2 mixtures can be generated in Ar matrices, experiments with pure CO were initially explored.[19] For example, under Cu/CO $\simeq 1/10^4$ conditions, a purple-colored, paramagnetic, 17-electron $Cu(CO)_3$ complex was generated and characterized by $^{12}C^{16}O/^{13}C^{16}O$ infrared isotopic substitution experiments as well as ultraviolet–visible and ESR spectroscopy.[19,20] A planar D_{3h} geometry was assigned to $Cu(CO)_3$ with a $^2A_2''$ electronic ground state in which the unpaired electron is localized in a $Cu(4p_z) + CO(2\pi)$ orbital combination.[19,20]

By experimenting with Cu/CO $\simeq 1/10^4-1/10^2$ mixtures it proved possible to generate the copper–copper bonded complex $Cu_2(CO)_6$[19] which could also be produced by annealing matrices containing the parent complex $Cu(CO)_3$:

$$\mathrm{Cu/CO} \xrightarrow[1/10^4-1/10^2]{10\ \mathrm{K}} \underset{\text{(yellow)}}{\mathrm{Cu_2(CO)_6}} \xleftarrow{40-45\ \mathrm{K}} \underset{\text{(purple)}}{\mathrm{2Cu(CO)_3}}$$

The dimerization reaction was monitored by quantitative IR/ultraviolet–visible/ESR spectroscopy.[19,20]

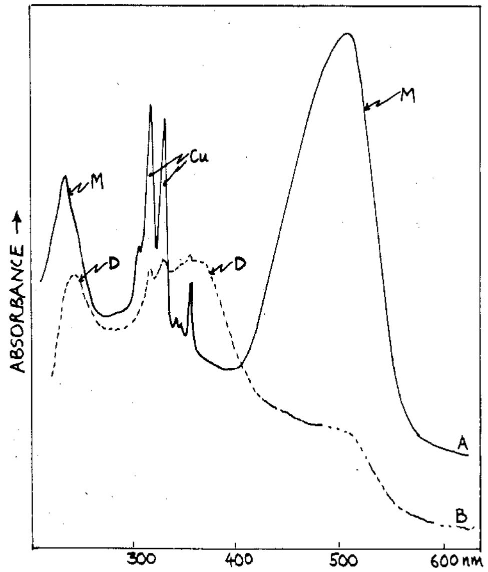

Figure 10. The ultraviolet–visible spectrum of the products of the $Cu/C_2H_4 \simeq 1/10^4$ cocondensation reaction (A) at 10 K showing $(C_2H_4)_3Cu$ (M) and (B) after warm-up to 50 K showing the growth of the 365/240 nm absorptions of $(C_2H_4)_{4,6}Cu_2$ (D).

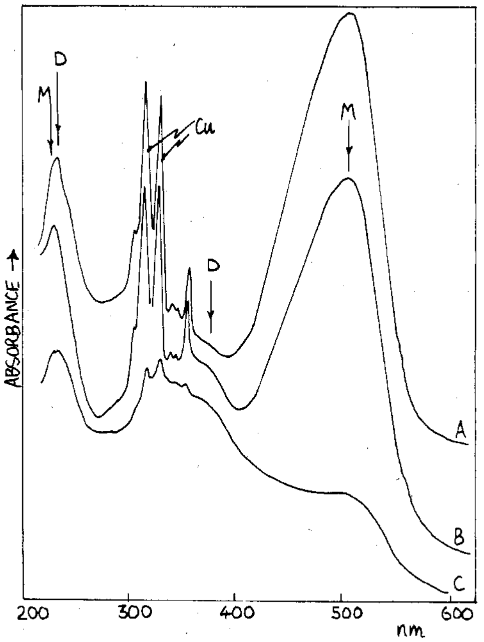

Figure 11. The ultraviolet–visible spectra of the products of the Cu/C_2H_4 matrix cocondensation reaction at 10 K: (A) $Cu/C_2H_4 \simeq 1/10^4$, (B) $Cu/C_2H_4 \simeq 1/10^3$, (C) $Cu/C_2H_4 \simeq 1/10^2$ showing $(C_2H_4)_3Cu$ (M) and $(C_2H_4)_{4,6}Cu_2$ (D).

The success of these experiments suggests an analogous route to binuclear, binary copper–ethylene complexes through the 17-electron, amber-colored, tris(ethylene) copper complex $(C_2H_4)_3Cu$ of the present study. Support for these proposals and convincing evidence for the existence of $(C_2H_4)_mCu_2$ (where $m = 4$ and/or 6) stems from two types of experimental observation. First, when $Cu/C_2H_4 \simeq 1/10^4$ matrices containing $(C_2H_4)_nCu$ (where $n = 2, 3$) are annealed at 50 K, the visible absorption around 505 nm gradually decays to zero with the concomitant growth of intense UV bands around 365 and 240 nm (Figure 10), a similar situation to that experienced with $Cu_2(CO)_6$ (417/287 nm). Second, the new complex giving rise to the 365/240-nm bands can also be generated by quantitative $Cu/C_2H_4 \simeq 1/10^4-1/10^2$ concentration experiments (Figure 11) from which a log $[A_D^{365}/A_M^{505}]$ vs. log $[Cu_0]$ plot (where A_D^{365} = absorbance of the 365-nm cluster band; A_M^{505} = absorbance of the 505-nm $(C_2H_4)_3Cu$ band; $[Cu_0]$ = Cu/Ar ratio) yields a slope of 0.98, the theory predicting unity[9,18,19,20] (Figure 12). These data provide convincing evidence for the binuclear nature of the new complex[9,18-20] and an argument in favor of the reaction sequence:

$$\mathrm{Cu/C_2H_4} \xrightarrow[1/10^4-1/10^2]{10\ \mathrm{K}} \mathrm{(C_2H_4)_{4,6}Cu_2} \xleftarrow{35-50\ \mathrm{K}} \mathrm{2(C_2H_4)_{2,3}Cu}$$

One can therefore tentatively associate the 365-nm absorption

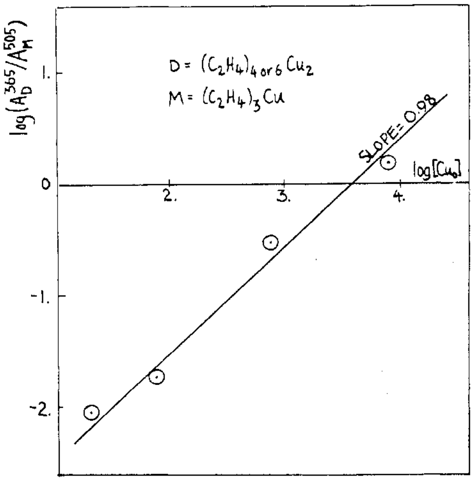

Figure 12. Graphical plot of the absorbance ratio log $[A_D^{365}/A_M^{505}]$ vs. log [Cu_0] proving that D is best formulated as a binuclear complex.

of $(C_2H_4)_{4,6}Cu_2$ with the $\sigma \rightarrow \sigma^*$ transition localized between orbitals associated mainly with the copper–copper bond,[21] while the 240-nm transition is probably analogous to the 235-nm MLCT transition of $(C_2H_4)_3Cu$. These assignments lead one to the interesting σ–σ^* tabulation (molecule, nm): Cu_2, 380–400; $Cu_2(CO)_6$, 417; $Cu_2(C_2H_4)_{6,4}$, 365. If these σ–σ^* energies can be taken as a measure of the strength of the copper–copper interaction (by analogy with the work on M–M bonded carbonyl complexes[21]), then one is led to believe that the copper–copper bond dissociation energy (or bond stretching force constant) order should follow $Cu_2(C_2H_4)_{4,6} > Cu_2 > Cu_2(CO)_6$.

Infrared Experiments. Binuclears. Presumably because of the weak copper–ethylene interaction, the dimerization studies of $(C_2H_4)_nCu$, as monitored by infrared spectroscopy, are not as revealing as the corresponding ultraviolet–visible experiments (Figures 3 and 4). This is reasonable, however, on the grounds that a major electronic perturbation is anticipated on passing from a paramagnetic (highly colored) $(C_2H_4)_nCu$ complex to the respective diamagnetic, binuclear $(C_2H_4)_mCu_2$. On the other hand, the alterations of the already weak copper–ethylene interaction are expected to be small and should have only a minimal effect on the corresponding vibrational frequencies. This proposal is borne out in practice as witnessed by the small, yet detectable, ν (C=C) and $\delta(CH_2)$ frequency shifts on passing from mononuclear to binuclear experimental conditions (see, for example, Figures 3 and 4).

The Nature of the Thermal Decomposition of $(C_2H_4)_nCu$ and $(C_2H_4)_mCu_2$. Evidence for the Growth of Small Copper Clusters. In the previous section we described two methods by which $(C_2H_4)_nCu$ (where n = 2 or 3) can be induced to dimerize to $(C_2H_4)_mCu_2$ (where m = 4 or 6). This process was monitored by infrared and ultraviolet–visible spectroscopy in the range 35–45 K for C_2H_4/Ar and 35–50 K for C_2H_4 matrices. Because of the pronounced tendency for copper–ethylene complexes to dimerize, it is meaningless to discuss the relative thermal stabilities of $(C_2H_4)_nCu$ and $(C_2H_4)_nNi$ complexes based on matrix warm-up data alone. However, the effect of warming $(C_2H_4)_mCu_2$ in the temperature range above 50 K deserves special mention as some rather remarkable ultraviolet–visible spectral effects develop which appear to be characteristic of *ethylene dissociation* and *controlled copper clustering*.[33] In the case of solid C_2H_4 containing $(C_2H_4)_{4,6}Cu_2$, the matrices could be warmed to just below the melting point of solid ethylene (104 K) under which circumstances the Cu_n clusters can still be considered to be reasonably well isolated (Figure 13A–C). During these controlled annealing experiments in C_2H_4, small copper clusters appear to be growing from Cu_n (where n = 2) to a Cu_n size regime where they are beginning to display optical properties characteristic of n = 2–5. We cannot, however, determine the size–frequency distribution of the Cu_n clusters from the existing data, and clearly a mixture exists. Copper-concentration studies designed to establish values of $n > 2$ would prove useful here and will form the basis of future research.[40] To achieve more extensive Cu_n aggregation than that attained in the C_2H_4 matrix experiments (Figure 13A–C) we have extended the $(C_2H_4)_{4,6}Cu_2$ decomposition technique to include concentrated C_2H_4/Ar matrices. Under these conditions the Ar begins to evaporate from the C_2H_4/Ar solid around 40–50 K, $(C_2H_4)_{4,6}Cu_2$ decomposition ensues around 45 K, and nucleation and copper cluster growth are observed upward from 45 K. A typical series of optical data for the aggregation phenomenon in $C_2H_4/Ar = 1/10$ is shown in Figure 13D–G. Immediately apparent under these lower temperature yet "less effective isolation conditions" is evidence for extensive Cu_n cluster growth but significantly to a nucleation stage which surpasses the peak size distribution realized from $(C_2H_4)_{4,6}Cu_2$ decompositions in C_2H_4.

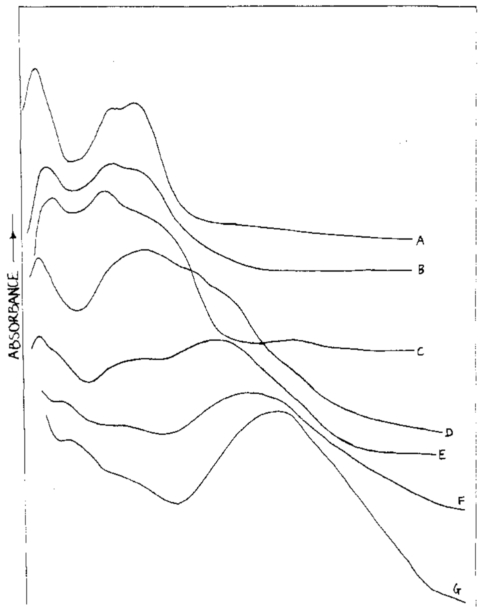

Figure 13. The optical spectra of the products of the decomposition of $(C_2H_4)_mCu_2$: (A–C) warmed up from 50 to 100 K from pure C_2H_4 matrices; (D–G) warmed up from 45 to 70 K from concentrated $C_2H_4/Ar \simeq 1/10$ matrices, showing the temperature–time evolution of "growing" copper clusters in the size regime less than 10 Å.

At this point we wish to emphasize the interconnection between our matrix approach of thermally decomposing labile copper–ethylene complexes in solid ethylene as a route to very small copper clusters (<10 Å) and Klabunde's metal atom–solvent (−196 °C) slurry technique (which is purported to involve "solvated metal atoms", i.e., weakly bound M(solvent)$_n$ complexes) as a synthetic pathway to supported or unsupported, highly dispersed, active particle catalysts.[35]

The optical properties of the decomposition products (illustrated in Figure 13) generally show *red* shifting absorptions (from roughly 350 to 600 nm) and concomitant bandwidth enlargement with increasing warm-up temperature (and presumably copper-cluster size) in the range 45 to 100 K. The properties of these spectra (especially those in Figure 13D-G) appear at first glance to be characteristic of massive copper clusters[22] rather than a superposition of electronic transitions of small copper clusters Cu_n intermediate in size between dimer and the bulk metal. However, at which cluster size one draws the line between a molecular Cu_n cluster optical spectrum and that of a plasma resonance spectrum (collective oscillation of the conduction electrons) of Cu_n microcrystallites is a point that remains to be settled. Certainly, the effects that we observe can readily be rationalized in terms of the Maxwell-Garnett theory[22] of the optical properties of small (with respect to the wavelength of light), spherical, metallic islands, modified to take account of changing cluster size. Similar effects have been observed for small Ag_n clusters.[38,39]

However, we also note that semiempirical molecular orbital treatments of Cu_n (and Ag_n) clusters[23] predict *linear* chains over both two- and three-dimensional structures for small Cu_n (and Ag_n) clusters. Particularly relevant to our observations is the fact that the *energy gap* between the HOMO and LUMO, as a function of cluster size for linear Cu_n (and Ag_n) aggregates, decreases monotonically, with IP's and EA's converging close to the work function of bulk copper (or silver). The calculations therefore predict a *long wavelength* shift in light absorption as particle size increases.[23] We wish to emphasize that this is *precisely the trend* which we observe experimentally for our proposed Cu_n clusters generated by controlled $(C_2H_4)_mCu_2$ decomposition (Figure 13).

Whether we have been fortunate enough to observe the optical spectra of "growing" Cu_n clusters in a size range appropriate for molecular orbital rationalizations of electronic properties[24] or whether the Cu_n clusters have reached the dimensions (size domain) where the optical spectra are more correctly treated in terms of Mie's general theory for light scattering and absorption by metallic spheres of varying "colloidal" dimensions[22] is a mute point and one that deserves further theoretical attention.

$(C_2H_4)_nCu$ and $(C_2H_4)_mCu_2$, Localized Bonding Models for Ethylene Chemisorbed onto Bulk Copper. In the context of ethylene chemisorption onto bulk copper, the UPS experiments of Demuth[4c] and Yu et al.[4d] are most enlightening in terms of the geometry of the adsorbent and the nature of the surface copper–ethylene bond. For example, Demuth[4c] recently demonstrated that it is possible to estimate the molecular geometry of adsorbed ethylene, from comparisons of the relative photoemission ionization energies with Hartree–Fock ground-state energies for distorted ethylene calculated using an SCF–LCAO method.

Demuth calculated that only weak distortions of the planar ethylene skeleton occurred for copper, in line with the small heat of adsorption for ethylene on copper and the fact that ethylene desorbs from copper at room temperature.[4] From earlier UPS studies of Demuth and Eastman[4e] it was anticipated that a correlation might exist between the observed π-level shifts for ethylene chemisorbed onto a series of metals and their respective heats of adsorption. Recently, however, Yu et al.[4d] showed that this was not in fact the case for Fe, Ni, and Cu, where the trend in the π-level shifts was actually in the *opposite* sense to corresponding chemisorption energies. Thus while the evidence for π–d surface bonding is now considered to be overwhelming,[4] the theory behind the analysis of surface UPS data will probably require modification to take into account the possibility of different "relaxation shifts" for the bonding π orbitals compared to nonbonding σ orbitals.[4] It is in this area of adsorbate–adsorbent interactions that we believe localized bonding models of the chemisorbed state can play a significant role.[3a,25] For example, we recently reported details of metal atom cryosynthetic techniques for generating "single-site representations" of the π-chemisorbed form of ethylene on group 8 metals, in the form of $(C_2H_4)Ni$[8b] and $(C_2H_4)Pd$.[14] The vibrational and electronic spectral data for such transition metal fragments are of central concern to those interested in probing metal–ligand interactions which have a logical relationship to problems in chemisorption and catalysis.[3,25] Recent successes with "multisite-representations" of the π-surface alkene bond include the metal atom syntheses of $(C_2H_4)Ni_2$ and $(C_2H_4)Ni_3$;[26] $(C_2H_4)_nCu$ and $(C_2H_4)_mCu_2$ of the present study can therefore be considered as a further step in the quest for localized bonding models of chemisorbed alkenes. Spectroscopically there is no obvious reason to formulate $(C_2H_4)_nCu/(C_2H_4)_mCu_2$ in any way other than normal π-alkene complexes. The weakness of the copper(0)–ethylene bond is certainly indicated by the facile thermal decomposition of $(C_2H_4)_mCu_2$ in the range 35 to 60 K. This temperature should be compared with the approximate decomposition temperatures 190, 273, and 300 K for $(C_2H_4)_3Pd$,[14,27] $(C_2H_4)_3Ni$,[8] and $(C_2H_4)_3Pt$,[7,27] respectively.

Interestingly, this stability order for our proposed localized bonding models of C_2H_4 on bulk Cu, Ni, Pd, and Pt parallels the respective heats of adsorption as well as the average UPS relaxation shifts.[4] Presumably these properties are partly reflective of the strength of the π–d surface interaction energy. In this context Demuth[4c] showed that stronger distortions of the sp^2 planar, carbon–hydrogen ethylene skeleton toward sp^3 hybridization occurred on Pd and Pt substrates which is to be contrasted with the weakly distorted (almost planar) ethylene chemisorbed on Ni[34] and Cu. The stronger distortions on Pt and Pd vs. Ni and Cu have been attributed to greater $d \rightarrow \pi^*$ back-bonding components of a stronger π–d surface interaction.[4c] Clearly, similar bonding arguments can be put forward to rationalize the thermal stability and metal–ethylene bond strengths of the proposed localized bonding models $(C_2H_4)_3M$ (where M = Cu, Ni, Pd, Pt). We note finally that C_2H_4 desorbs at room temperature from Cu[4] indicating a fairly weak binding energy. This is in line with the 35–60 K decomposition range for $(C_2H_4)_mCu_2$. In contrast C_2H_4 on Ni dehydrogenates spontaneously into C_2H_2 and H_2 at room temperature,[4c–e] whereas $(C_2H_4)_3Ni$ is purported to decompose at 0 °C to ethylene and metallic nickel.[8a] This striking difference between the "finite" complex and the "infinite" surface analogue convincingly demonstrates the prerequisite of at least two metal sites for alkene dehydrogenation on bulk nickel and is an interesting case where metal cluster–metal surface analogies and localized bonding concepts must be carefully scrutinized.

Acknowledgment. This research was completed while G. A. O. was a Sherman-Fairchild Distinguished Scholar (1977) at California Institute of Technology. The hospitality of the Chemistry Division of Caltech is greatly appreciated. We gratefully acknowledge the financial assistance of the National Research Council of Canada, the Atkinson Foundation, the Connaught Foundation, Imperial Oil, Erindale College, and the Lash Miller Chemistry Laboratory. An NRCC graduate scholarship (for D.M.) is also greatly appreciated.

Registry No. I, 60203-82-9; II, 60241-41-0; III, 60203-83-0; $(C_2H_4)_4Cu_2$, 64091-84-5; $(C_2H_4)_6Cu_2$, 64091-83-4; $(^{13}C_2H_4)Cu$, 64091-80-1; $(^{12}C_2H_4)(^{13}C_2H_4)Cu$, 64091-79-8; $(^{13}C_2H_4)_2Cu$, 64091-78-7.

References and Notes

(1) (a) R. G. Salomen and J. K. Kochi, *J. Am. Chem. Soc.*, **95**, 1889 (1973); (b) J. K. Hurst and R. H. Lane, *ibid.*, **95**, 1703 (1973); (c) D. Meyerstein, *Inorg. Chem.*, **14**, 1716 (1975), and references cited therein.

(2) (a) D. Schwendiman and C. Kutal, *Inorg. Chem.*, **16**, 719 (1977); (b) M. Wrighton, *Chem. Rev.*, **74**, 401 (1974), and references cited therein.

(3) (a) G. A. Ozin, *Acc. Chem. Res.*, **10**, 21 (1977); (b) E. L. Muetterties, *Bull. Soc. Chim. Belg.*, **84**, 959 (1975); *Science*, **196**, 839 (1977); (c) R. Ugo, *Catal. Rev.*, **11**, 225 (1975).

(4) (a) D. O. Hayward and B. M. W. Trapnell, "Chemisorption", Butterworths, Washington, D.C., 1974; (b) R. P. Eischens, W. A. Pliskin, and S. A. Frances, *J. Chem. Phys.*, **22**, 1786 (1954); (c) J. E. Demuth, *Surf. Sci.*, in press (private communication); (d) K. Y. Yu, W. E. Spicer, I. Lindau, P. Pianetta, and S. F. Lin, *ibid.*, **57**, 157 (1976); *Spec. Period Rep.*, **5**, 103 (1976); (e) J. E. Demuth and D. E. Eastman, *Phys. Rev. B*, **13**, 1523 (1976), and references cited therein.

(5) H. Huber, D. McIntosh, and G. A. Ozin, *J. Organomet. Chem.*, **C50**, 112 (1976).

(6) (a) E. P. Kündig, M. Moskovitis, and G. A. Ozin, *J. Mol. Struct.*, **14**, 137 (1972); (b) M. Moskovits and G. A. Ozin, *J. Appl. Spectrosc. (Engl. Transl.)*, **26**, 487 (1972).

(7) P. L. Timms, communicated in a paper given at the C.I.C. Meeting "Chemistry under Extreme Conditions", Toronto, June 1975.

(8) (a) K. Fischer, K. Jonas, and G. Wilke, *Angew. Chem., Int. Ed. Engl.*, **12**, 565 (1973); (b) H. Huber, G. A. Ozin, and W. J. Power, *J. Am. Chem.* Soc., **98**, 6508 (1976).

(9) E. P. Kündig, M. Moskovits, and G. A. Ozin, *Angew. Chem., Int. Ed. Engl.*, **14**, 292 (1975); M. Moskovits and J. Hulse, *J. Chem. Soc., Faraday Trans. 2*, 471 (1977).

(10) D. McIntosh and G. A. Ozin, *J. Organomet. Chem.*, **121**, 127 (1976).

(11) M. Green, J. A. K. Howard, J. L. Spencer, and F. G. A. Stone, *J. Chem. Soc., Chem. Commun.*, 449 (1975).

(12) (a) C. Kruger and Y.-H. Tsay, Abstracts of the 6th International Conference on Organometallic Chemistry, Amherst, 1973, p 80; (b) M. Green, J. A. K. Howard, J. L. Spencer, and F. G. A. Stone, *J. Chem. Soc., Dalton Trans.*, **271** (1974).

(13) N. Rosch and R. Hoffman, *Inorg. Chem.*, **13**, 2656 (1974).

(14) H. Huber, G. A. Ozin, and W. J. Power, *Inorg. Chem.*, **16**, 979 (1977).

(15) (a) T. Ogura, *Inorg. Chem.*, **15**, 2301 (1976); (b) G. V. Buxton, J. C. Green, and R. M. Sellers, *J. Chem. Soc., Dalton Trans.*, 2160 (1976).

(16) R. P. Messmer, "The Physical Basis of Heterogeneous Catalysis", E. Drauglis and R. K. Jaffee, Ed., Plenum Press, New York, N.Y., 1975.

(17) (a) R. G. Denning, F. R. Hartley, and L. M. Venanzi, *J. Chem. Soc. A*, 1322 (1967); (b) D. J. Trecker, J. P. Henry, and J. E. McKean, *J. Am. Chem. Soc.*, **87**, 3261 (1965); (c) T. N. Murrel and S. Carter, *J. Chem. Soc.*, 6185 (1964).

(18) G. A. Ozin, *Appl. Spectrosc.*, **30**, 573 (1976).

(19) H. Huber, E. P. Kündig, M. Moskovits, and G A Ozin, *J. Am. Chem. Soc.*, **97**, 2097 (1975).

(20) M. Moskovits and G. A. Ozin, "Cryochemistry", Wiley, New York, N.Y., 1976; B. McGarvey and G. A. Ozin, unpublished work.

(21) (a) R. A. Levenson, H. B. Gray, and G. P. Ceasar, *J. Am. Chem. Soc.*, **92**, 3653 (1970); (b) J. P. Fawcett, A. J. Poe, and M. V. Twigg, *J. Chem. Soc., Chem. Commun.*, 267 (1973); (c) M. Wrighton and D. Bredesen, *J. Organomet. Chem.*, **C35**, 50 (1973).

(22) (a) J. C. Maxwell-Garnett, *Phil. Trans. R. Soc.*, **203**, 385 (1904); **205**, 237 (1906); (b) G. Mie, *Ann. Phys. (Leipzig)*, **25**, 377 (1908); (c) R. H. Doremus, *J. Appl. Phys.*, **37**, 2775 (1966), and references cited therein; (d) O. Hunderi and R. Ryberg, *J. Phys. F.*, in press (private communication).

(23) (a) R. C. Baetzold, *J. Chem. Phys.*, **55**, 4363 (1971); *J. Catal.*, **29**, 129 (1973); *Adv. Catal.*, **51**, 1 (1975); (b) R. C. Baetzold and R. E. Mack, *J. Chem. Phys.*, **62**, 1513 (1975), and references cited therein.

(24) R. P. Messmer, S. K. Knudsen, K. Johnson, J. B. Diamond, and C. Y. Yang, *Phys. Rev. B*, **13**, 1396 (1976), and references cited therein.

(25) G. A. Ozin, *Catal. Rev.*, in press, and references cited therein.

(26) G. A. Ozin, W. J. Power, W. A. Goddard III, and T. Upton, submitted for publication in *J. Am. Chem. Soc.*

(27) R. M. Atkins, R. McKenzie, P. L. Timms, and T. W. Turney, *Chem. Commun.*, 764 (1975).

(28) (a) D. C. Andrews, G. Davidson, and D. A. Duce, *J. Organomet. Chem.*, **101**, 113 (1975); (b) D. B. Powell and N. Sheppard, *J. Chem. Soc.*, 2519 (1960); (c) J. Hiraishi, *Spectrochim. Acta, Part A*, **25**, 749 (1969); (d) D. B. Powell, J. G. V. Scott, and N. Sheppard, *ibid.*, **25**, 327 (1972); (e) M. J. Grogan and K. Nakamoto, *J. Am. Chem. Soc.*, **88**, 5454 (1966).

(29) L. Brewer and B. King, *J. Chem. Phys.*, **53**, 3981 (1970), and references cited therein.

(30) G. A. Ozin and D. McIntosh, in preparation.

(31) The existence and predominance of the 15-electron coordinatively unsaturated complex $(C_2H_4)_2Cu$ together with the 17-e complex $(C_2H_4)_3Cu$ in pure C_2H_4 matrices as well as concentrated C_2H_4/Ar matrices were shown *not* to be a photochemical artifact of the type $(C_2H_4)_3Cu \rightarrow (C_2H_4)_2Cu + C_2H_4$ ($h\nu$) caused by ultraviolet–visible radiation accompanying the infrared radiation from the Nernst glower by (1) recording spectral data with and without a germanium cut-out filter in the IR sample beam, (2) searching for time-dependent changes in the infrared spectra, and (3) performing intentional UV–visible photolyses of $(C_2H_4)_nCu$.[36] In the context of the present discussion the results were negative, implying that the coexistence of $(C_2H_4)_{2,3}Cu$ in pure C_2H_4 matrices (and apparent preference for $(C_2H_4)_2Cu$) is probably another case of a lattice site symmetry restriction effect of the type observed previously for $(C_2H_4)_{2,3}Ni$.[8b] In brief, the C_{2h} lattice substitutional site of solid ethylene favors the "twofold" structural property of a $(C_2H_4)_2Cu$ complex and tends to impede formation of the "threefold" type $(C_2H_4)_3Cu$ complex. The reader is referred to ref 8b for a detailed discussion of this effect.

(32) The 1164/1155-cm^{-1} band splitting is especially sensitive to the deposition conditions and can also appear as a shifted doublet at 1156/1138 cm^{-1} and is attributed to a matrix site and/or multiple trapping site effect (see later).

(33) Whether or not the ethylene is weakly chemisorbed to these copper clusters is an interesting point but one that cannot readily be ascertained from our conventional transmission infrared techniques, especially as the vibrational spectrum of weakly bonded C_2H_4 on bulk copper is likely to be only slightly perturbed from that of free ethylene.

(34) GVB–CI molecular orbital calculations for $Ni(C_2H_4)$ and $Ni_2(C_2H_4)$ convincingly support this view.[26]

(35) K. J. Klabunde, H. F. Efner, T. O. Murdock, and R. Ropple, *J. Am. Chem. Soc.*, **98**, 1021 (1976).

(36) H. Huber and G. A. Ozin, unpublished work.

(37) We have recently completed a series of spin-restricted SCF–Xα–SW transition-state molecular orbital calculations for the group 1B complexes $(C_2H_4)M$ (where M = Cu, Ag, Au). These provide convincing support for our spectral assignments as well as a rationale for the ultraviolet and visible charge-transfer spectral shifts on passing from Cu to Ag to Au:[10] D. McIntosh, R. P. Messmer, and G. A. Ozin, in preparation.

(38) H. Huber and G. A. Ozin, *Inorg. Chem.*, in press.

(39) W. Schulze, H. U. Becker, and H. Abe, "International conference on Matrix Isolation Spectroscopy", West Berlin, June 1977, paper 8.5.

(40) S. Mitchel and G. A. Ozin, in preparation.